Analysis of Pile Foundations Under Dynamic Loads

G. Waas, H.-G. Hartmann
Hochtief AG., Abt. Kerntechnischer Ingenieurbau,
Bockenheimer Landstr. 24, D-6000 Frankfurt/Main 1, Germany

A method is presented for the analysis of pile foundations which are subjected to horizontal dynamic loads from earthquakes, airplane impact, gas explosion or other sources. The motion of the pile cap and the pile forces are computed. - The loads may be applied to the pile cap or directly to the piles (e.g. by earthquake wave motion). The soil may be stratified and is considered to be an elastic or visco-elastic medium. The piles are assumed vertical.

The method makes use of an approximate fundamental solution for displacements caused by a dynamic point load in a layered visco-elastic medium. The approximation involves a discretization of the medium in the vertical direction. In horizontal directions the medium is treated by continuum theory. The soil medium supports each pile at about 10 to 20 nodes. A dynamic flexibility matrix for the soil is derived which relates the elastic, damping and inertial forces of the soil to the displacements at each node. It includes effects of radiation damping. All piles are coupled through the soil flexibility matrix. The piles are modelled by beam elements. Transient response is computed using fast discrete Fourier transforms.

The arrangementof the piles is arbitrary. However, simple and double symmetry can be accounted for by the computer program. When the pile arrangement is axisymmetric, the degrees of freedom can be reduced to only those of two piles per ring.

The influence of the number of piles and the influence of the pile spacing on group stiffness and on pile forces is presented for two soil profiles. Dynamic effects on pile forces of a foundation for a reactor building are studied. They are significant when soils are soft.

1. Introduction

Pile foundations of nuclear power plant structures have to withstand substantial dynamic loads which may be caused by earthquakes, the impact of a crashing airplane or a gas cloud explosion. While vertical dynamic loads usually pose no major problems, horizontal dynamic loads may govern the design, because piles are well suited to carry vertical loads, but are relatively weak when strained horizontally. During recent, small and moderate earthquakes in Japan, many pile foundations were damaged. This indicates a general susceptibility of pile foundations to ground shaking.

The theoretical and empirical knowledge on the dynamic response of pile groups is rather limited. The method presented below provides a tool for analysis. It is basically similar to the method Wolf /1/ has presented, but appears to be somewhat more elegant and efficient. The method is used to study the response of a group of vertical piles to dynamic horizontal loads, as indicated in Fig. 1.

2. Method of Analysis

Purpose:

Displacements, shear forces and bending moments shall be computed for a group of piles which are subjected to horizontal loads. The loads may be static or dynamic forces, prescribed displacements or accelerations. Pile-soil-pile interaction is taken into account.

Assumptions:

The soil is horizontally layered; it extends laterally to infinity and is underlain by a rigid base at a finite depth. The soil is treated as a linear elastic or visco-elastic medium using complex modulus representation. Non-linear soil behavior may be approximated by adjusting iteratively the moduli and damping values to computed strain levels in each soil layer.

The piles consist of vertical beam elements with linear bending and shear behavior including material damping. The location of the piles in plan is arbitrary. Symmetry properties may be utilized to reduce the required storage and computational effort. The piles are pinned or fixed at the pile cap which is assumed rigid for simplicity.

Procedure:

Each pile is connected to the soil at several, say 10 to 20, nodes or rather nodal rings, as indicated in Figs. 1 and 2. Horizontal displacements and rotations of the soil and the piles are matched at these nodal rings and equilibrium is enforced. To this end, soil and piles are considered as substructures. First, the displacement field caused by time harmonic ring loads in a layered visco-elastic medium, see Fig. 3, is computed as outlined in the appendix. The displacements of the soil are then evaluated for the nodes of all the piles to form the frequency dependent dynamic flexibility matrix of the soil, F_s. In doing so, point loads are used rather than ring loads when flexibility terms are computed that relate forces and displacements of different piles. Vertical displacements in the soil caused by horizontal loads are disregarded to reduce the complexity of the problem.

Next, the flexibility matrix of the piles, F_p, is computed. Finally, soil and piles are connected leading to:

$$(F_s + F_p)\, P_i = F_p\, P_e \qquad (1)$$

with

$$F_p\, (P_e - P_i) = u \qquad (2)$$

and

$$F_s\, P_i = u \qquad (3)$$

where P_e = external loads, P_i = internal forces between soil and piles, and u = displacements of pile nodes. Matrices and vectors are complex valued, representing amplitudes and phases of harmonic motion at given frequency. F_s includes radiation and material damping as well as inertia forces of the soil. F_p may include damping and inertia forces of pile and pile cap mass.

Computation of pile forces and modification of Eqs. 1 to 3 for prescribed displacements or accelerations follows standard procedures. - Earthquake excitation is incorporated through vertically propagating shear waves which are generated in the model by horizontal acceleration of the bottom boundary.

For axisymmetric pile arrangements the dimensions of P and u in Eqs. 1 to 3 can be reduced by Fourier expansion of P and u in the tangential direction, leading to only two degrees of freedom per pile ring and nodal depth.

The complete analysis of a group of 356 piles, shown in Fig. 4, with 11 nodes per pile took less than 30 seconds per frequency on a CDC Cyber 175.

3. Static Group Effects

Fig. 4 shows two groups of piles with diameter D = 1,3 m. The piles are fixed at a rigid pile cap. A soft and a relatively stiff soil profile are given. The lower sand layer extends to - 50 m and is underlain by rigid rock. The displayed average pile spacing in the group of 356 piles is d = 2,5 D.

Fig. 5 shows that the horizontal stiffnesses of the pile groups decrease with decreasing pile spacing, for the large group more so than for the small group. Results for piles pinned to the pile cap are very similar. With decreasing pile spacing, bending moments in the piles increase though the horizontal forces are kept constant, see Fig. 6.

4. Dynamic Effects

Fig. 7 shows that the dynamic stiffness of a single pile is hardly affected by the frequency of the motion, whereas that of a large group of piles may strongly depend on frequency. The resonant frequencies of the soil layers are excited by the large number of piles. Displayed results are for stiff soil conditions.

Transfer functions for the same soil conditions are presented in Fig 8. Those for a single pile hardly differ from that of the soil in the free field (without piles). However, 356 piles show significant interaction with the soil and reduce resonant peaks. When building mass is added, the resonant frequency may drop below that of the free field soil motion and radiation damping is lost.

Transfer functions from rock motion to shear forces and bending moments in the piles are very similar to those from rock motion to the building mass and may be approximated by that of a simple damped oscillator. Rigorous time history analyses with fast numerical Fourier transformations have shown good agreement in computed pile forces with an approximate analysis in which pile forces were computed for rock motion at only one frequency close to resonance or below. The maximum base shear force of the building has to be matched, of course.

A quasi-static approach to compute earthquake induced shear forces and bending moments in piles by simply applying a static base shear force at the pile cap may underestimate the actual pile forces, especially in very soft soils. The inertia of the soil adds to the loading of the piles. A comparison of maximum pile forces computed dynamically with those

computed using a static base shear force applied at the pile cap is shown in Fig. 9 through 12 for stiff and soft soil conditions. For soft soil conditions the differences are remarkable. Note that shear forces may increase with depth in soft soil due to inertia forces of the soil. In stiff soil, peripheral piles may receive significantly larger shear forces and bending moments than interior piles.

5. Closure

The presented method is hoped to provide an efficient tool for further studies on pile group response to dynamic horizontal loads. It has been shown that the dynamic response of pile groups may be very different from that of individual piles and that quasi-static analyses may underestimate pile forces induced by earthquakes. A comparison of the analytical results with test results on pile groups is wanted to investigate the importance of non-linear effects.

References

/1/ Wolf, J.P. and von Arx, G.A., "Impedance Function of a Group of Vertical Piles," Earthquake Eng. and Soil Dynamics Conf., ASCE, Pasadena, Cal., June 1978.

/2/ Waas, G., "Linear Two-dimensional Analysis of Soil Dynamics Problems in Semi-infinite Layered Media", Diss., Univ. of Cal., Berkeley, 1972.

/3/ Waas, G., "Dynamisch belastete Fundamente auf geschichtetem Baugrund", VDI-Berichte Nr. 381, 1980.

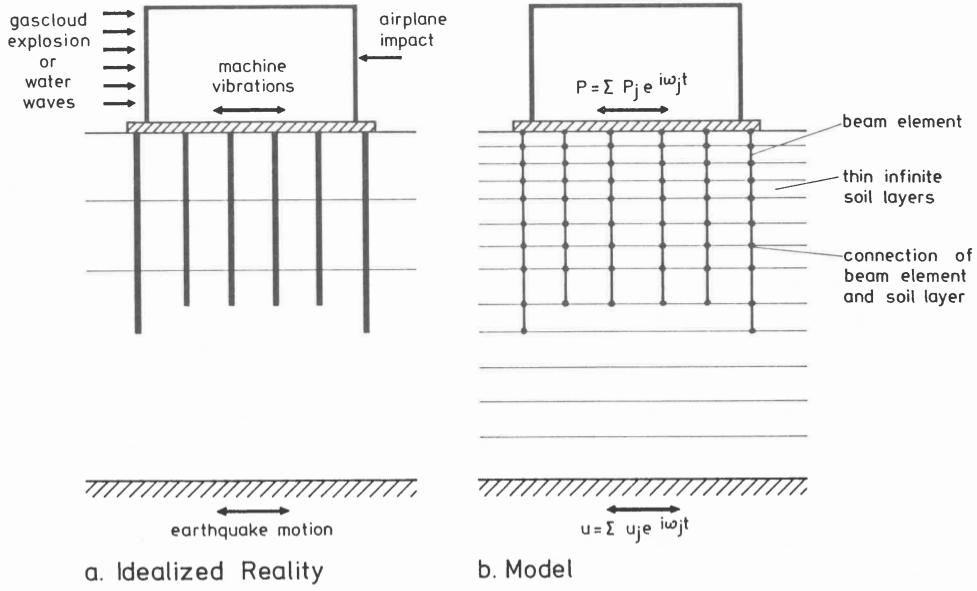

Fig. 1 Pile foundation subjected to horizontal dynamic loads

APPENDIX

Ring and Point Loads in a Layered Medium

The displacements of harmonic motion in a layered elastic or viscoelastic medium at frequency ω may be represented in cylindrical coordinates, Fig. 3, using the following functions:
$e^{i\omega t}$ for the variation in time,
$e^{i\nu\theta}$ for the variation in the hoop direction,
the Bessel functions J_ν (kr) or H_ν (kr) for the variation in the radial direction, and continuous piece wise linear functions in the z-direction. The functions in t, θ and r satisfy the respective ordinary differential equations, which are obtained by seperation of variables from the equations of motion in cylindrical coordinates. The functions in z are approximations which require a subdivision of the natural soil layers into thin layers as indicated in Fig. 3 /2/. The number of layers be n.

Enforcing compatibility of displacements and equilibrium at the interfaces of the n soil layers and observing homogeneous boundary conditions (zero stresses at top and zero displacements at bottom) yield two eigenvalue problems /2/ which can be solved easily. They depend on ω but are independent of ν. The homogeneous solution for motion in the r-z plane consist of 2 n generally complex wave numbers k_j and the eigenvectors X_j and Z_j containing the horizontal and vertical displacement components respectively. For motion in the r-θ plane one obtains n wave numbers $\bar{k}_j$ and the corresponding vectors Y_j.

The displacements u, v, w and the strains and stresses can now be expanded in terms of the eigensolutions. In order to compute the displacements caused by ring loads at distance R from the center line, see Fig. 3, one may consider a cylindrical surface at radius R. When computing displacements and stresses, one has to use the Bessel functions J_ν for $r \leq R$ due to the reflection at r = 0, and the Hankel function $H_\nu^{(2)}$ for $r \geq R$, because amplitudes must decay with distance from R /3/. At the cylindrical surface r = R, internal stresses and external loads must be in equilibrium and displacements must be compatible. Enforcement yields the following results:

The displacements at a point (r, z=l, θ) caused by a line load at the nodal ring (R, z=h), see Fig. 3, are

$$u = \left[\sum_{j=1}^{2n} H_j' X_{lj} a_j + \sum_{j=1}^{n} \frac{\nu}{r} \bar{H}_j Y_{lj} c_j\right] \cdot \frac{-i}{4} \cos \nu\theta \cdot e^{i\omega t} \qquad (1)$$

$$v = \left[\sum_{j=1}^{2n} \frac{\nu}{r} H_j X_{lj} a_j + \sum_{j=1}^{n} \bar{H}_j' Y_{lj} c_j\right] \cdot \frac{i}{4} \sin \nu\theta \cdot e^{i\omega t} \qquad (2)$$

$$w = \left[\sum_{j=1}^{2n} k_j H_j Z_{lj} a_j\right] \frac{-i}{4} \cos \nu\theta \cdot e^{i\omega t} \qquad (3)$$

$$H_j = H_\nu^{(2)}(k_j r); \quad H_j' = \frac{d}{dr} H_j; \quad \bar{H}_j = H_\nu^{(2)}(k_j r); \quad \bar{H}_j' = \frac{d}{dr} \bar{H}_j \tag{4}$$

For a ring load in r-direction $p_r = \cos\nu\theta/2\pi R$

$$a_j = J_j' X_{hj} \qquad c_j = \bar{J}_j Y_{hj} \frac{\nu}{R} \tag{5}$$

For a ring load in θ-direction $p_\theta = -\sin\nu\theta/2\pi R$

$$a_j = J_j X_{hj} \frac{\nu}{R} \qquad c_j = \bar{J}_j' Y_{hj} \tag{6}$$

For a ring load in z-direction $p_z = \cos\nu\theta/2\pi R$

$$a_j = k_j J_j Z_{hj} \qquad c_j = o \tag{7}$$

Eqs. 1 to 7 are valid for $r \geq R$, for $r < R$ Hankel and Bessel functions must be interchanged. The abbreviations with J_j correspond to those in Eq. 4. Normalization of X_j, Y_j and Z_j is understood as in /2/ but with a subsequent division by k_j or $\bar{k}_j$, respectively.

When the radius R of the ring load goes to zero one obtains the displacements caused by a point load.

For a horizontal point load $P_x = 1$ in the x-direction ($\theta = o$) ν is one and

$$a_j = k_j X_{hj} \qquad c_j = \bar{k}_j Y_{hj} \tag{8}$$

For a vertical point load, $P_z = 1$, ν is zero and

$$a_j = k_j Z_{hj} \qquad c_j = o \tag{9}$$

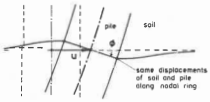

Fig. 2 Connection between pile and soil at interfaces of thin soil layers

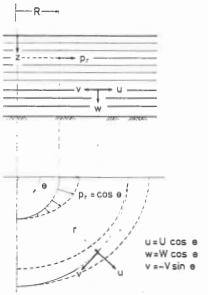

Fig. 3 Displacements in a horizontally layered medium caused by a horizontal ring load for $\nu = 1$

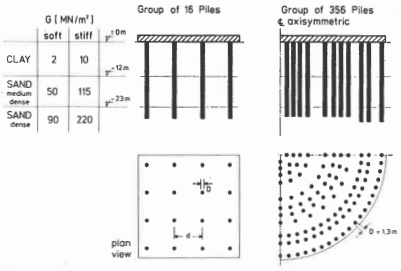

Fig. 4 Pile groups with 16 and 356 piles (total depth of model 50 m)

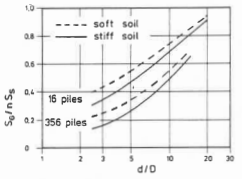

S_G = Horizontal stiffness of pilegroup
S_S = Horizontal stiffness of single pile
n = Number of piles

Fig. 5 Group efficiency for horizontal stiffness (pile heads fixed at pile cap)

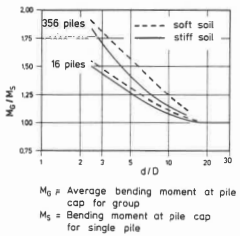

M_G = Average bending moment at pile cap for group
M_S = Bending moment at pile cap for single pile

Fig. 6 Group effect on bending moments for same average shear force at pile heads

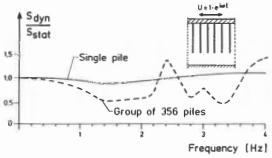

Fig. 7 Ratio of dynamic and static horizontal stiffness (absolute values)

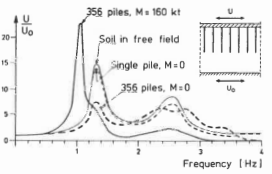

Fig. 8 Transfer functions from base motion to pile cap and soil surface motion (absolute values)

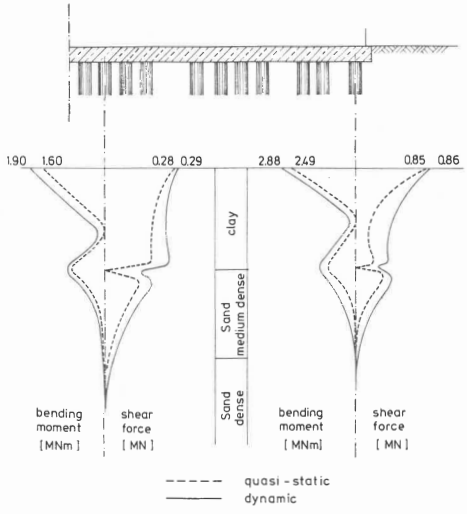

Fig. 9 Shear forces and bending moments in piles for stiff soil conditions

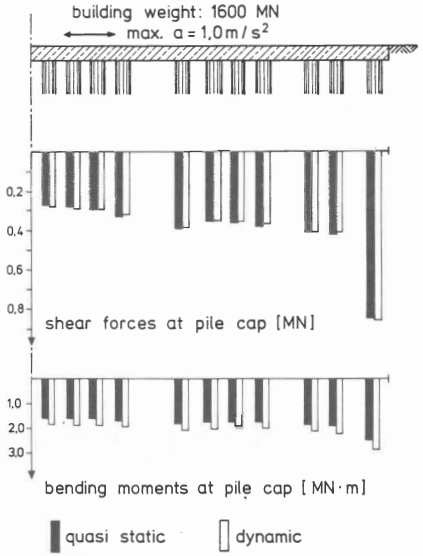

Fig. 10 Shear forces and bending moments of inner and outer piles for stiff soil (different scales)

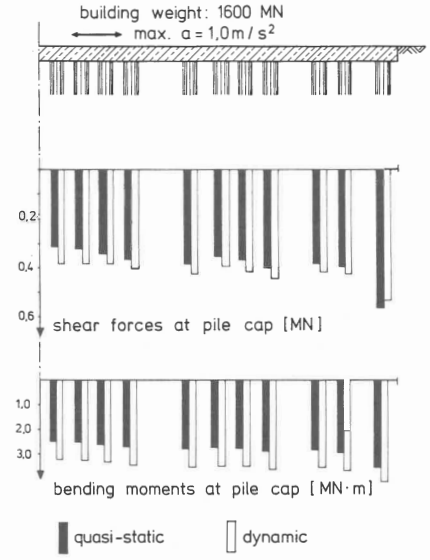

Fig. 11 Shear forces and bending moments in piles for soft soil conditions

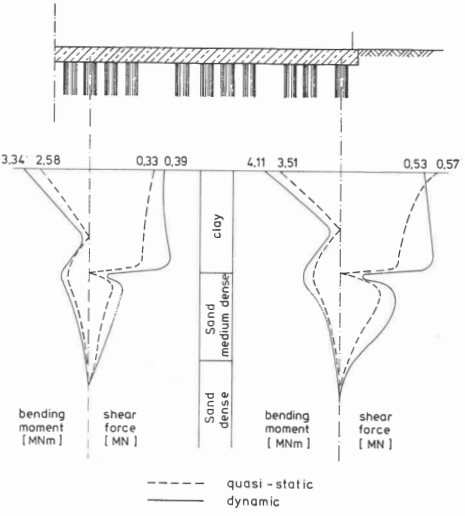

Fig. 12 Shear forces and bending moments of inner and outer piles for soft soil (different scales)